JOURNAL OF GEOPHYSICAL RESEARCH, VOL. 103, NO. D21, PAGES 28,079–28,092, NOVEMBER 20, 1998

Optical properties of Saharan dust during ACE 2

A. Smirnov,[1,2] B. N. Holben,[1] I. Slutsker,[1,2] E. J. Welton,[3] and P. Formenti[4]

Abstract. The Aerosol Robotic Network (AERONET) of automatic Sun/sky radiometers collected data on Tenerife, Canary Islands, in June-July 1997 during the second Aerosol Characterization Experiment (ACE 2). Initially, two instruments were deployed at Izana observatory (2360 m above sea level) and one at a mountain station Teide (3570 m above sea level). Repeatability of the calibration constants (Langley method) for all instruments was less than 0.5%. Aerosol optical depths measured by colocated sunphotometers and column size distributions, retrieved from spectral sky radiance data, were in good agreement. Later, one of the instruments was relocated at sea level. On July 8, 17, and 25, Saharan dust outbreaks were observed. Diurnal variations of spectral aerosol optical depth are presented. Relative diurnal stability of Saharan dust optical properties has been observed. Volume size distributions at various heights (sea level and 2360 m above sea level) show that the main portion of coarse particles is situated above 2360 m level. Measurements on July 25 showed how incoming dust has changed the magnitude and spectral dependence of aerosol optical depth and volume spectra of columnar aerosol. Mean optical depth and Angstrom parameter values for Saharan dust outbreaks during the ACE 2 experiment agree well with the Atlantic Ocean and Bermuda data obtained during the Tropospheric Aerosol Radiative Forcing Observational Experiment (TARFOX) in July 1996, as well as with previously reported Atlantic Ocean results. Also, there is a good agreement between ACE 2 data for Saharan air masses and data obtained on certain sites of the AERONET network.

1. Introduction

The Sahara desert region is one of the most extensive sources of mineral dust in the northern hemisphere [*Husar et al.*, 19971. Mineral dust, being considered as a part of natural background aerosol, often has been neglected in anthropogenic climate change considerations [*Andreae*, 19961. Although it is not presently possible to determine the entire influence of mineral dust on global climate, *Li et al.* [1996] suggest that it could be an important climate-forcing component over specific oceanic areas and other regions where dust concentrations are high. Saharan dust optical properties are important for various estimations of radiative forcing [*Tegen et al.*, 1996] inasmuch as dust plays an important role in radiative processes.

The second Aerosol Characterization Experiment (ACE 2) of the International Global Atmospheric Chemistry Project took place from June 16 through July 25, 1997. ACE 2 was designed to study the radiative effects of anthropogenic aerosols from Europe and desert dust from Africa as they are transported over the North Atlantic Ocean.

In this work we investigate aerosol optical properties of cloudless atmosphere derived from Sun and sky measurements. We analyze specific optical conditions and aerosol microstructure over Tenerife during Saharan dust oubreaks. We provide details on aerosol optical properties in total atmospheric column, complementing spatial in situ analysis of the dynamics of the atmospheric dust mass particle size distributions [*Arimoto et al.*, 1997].

2. Measurement Strategy

The Aerosol Robotic Network (AERONET) of automatic Sun/sky radiometers collected data on Tenerife, Canary Islands, in June-July 1997 during ACE 2. The instrument deployed in the network is an automatic **Sun** and sky scanning radiometer CIMEL CE-318. This instrument made measurements of the direct **Sun** radiances in seven spectral channels within the spectral range 340-1020 nm and sky radiances in four spectral channels *[Holben et al.*, 19981. The bandwidths of the interference filters employed in these radiometers varied from 2 to 10 nm. The ratio of transmittance in the wings to the maximum transmittance of the filters was less than 10^{-4}. CIMEL instruments are not temperature stabilized. Our measurements of the spectral temperature sensitivity of the instrument in a temperature-controlled chamber showed agreement with the manufacturers published temperature sensitivity of the detectors. However, the 1020 nm channels showed significant voltage temperature variation

[1] Biospheric Sciences Branch, NASA Goddard Space Flight Center, Greenbelt, Maryland.
[2] Also at Science Systems and Applications, Inc., Lanham, Maryland.
[3] Physics Department, University of Miami, Coral Gables, Florida.
[4] Biochemistry Department, Max Planck Institut fur Chemie, Mainz, Germany.

Paper number 98JD01930.
0148-0227/98/98JD-01930$09.00

Table 1. Variation Coefficients of the Canary-Derived Langley Spectral Extraterrestrial Voltages

	λ, nm						
	1020	870	670	440	500	380	340
CIMEL 2	0.004	0.002	0.003	0.003	0.002	0.004	0.011
CIMEL 13	0.004	0.004	0.002	0.005	0.004	0.006	0.008
CIMEL 55	0.003	0.002	0.001	0.005	--	--	--

(0.25%/°C ±0.05%/°C) warranting a correction to a reference temperature in the processing *[Holben et al.,* 19981.

High-altitude conditions at Izana observatory and at Teide station presented an opportunity for careful calibration of sunphotometers by the Langley method. Further deployment of one of the instruments at an elevation of 10 m above sea level enabled us to draw certain conclusions related to the vertical profiles of atmospheric optical parameters during Saharan dust outbreaks and in background conditions. These results can be used to complete column-closure experiments by comparing the radiation perturbations measured at various levels of the atmosphere with the corresponding simulations.

Two instruments (CIMEL 2 and CIMEL 13) were deployed at Izana observatory at the height 2360 m above sea level. Langley calibrations were made only during morning hours in the period from June 18 through July 25 with CIMEL 2 (28 Langley plots) and from June 17 through June 24 with CIMEL 13 (7 Langley plots). Performance of both instruments was satisfactory and coefficients of variation, defined as standard deviation divided by average of spectral extraterrestrial voltages, yielded values listed in Table 1. In the majority of channels, variation coefficients are smaller or equal to 0.5%, being slightly higher in the UV channels. During the overlapping time period (from June 18 through June 24) it became possible to make a comparison of two instruments.

Aerosol optical depths measured by colocated sunphotometers and column size distributions, retrieved from spectral sky radiance data, are in good agreement during the averaging period (Figures la and lb). Discrepancies between optical depths in the 670-1020 nm range are well below the accuracy of ± 0.01 *[Holben et al.,* 19981. Size distribution retrievals are consistent in the most reliable size range from 0.1 through 3 μm *[Kaufman et al.,* 19941. The latter conclusion simply emphasizes good agreement between measured and calculated sky radiances in the solar almucantar (the root-mean-square of the match is less than 2% for all four spectral channels), though actual difference in that retrieved size distributions could be higher.

In our analysis we will also employ optical depth data obtained at a mountain station Teide at the elevation 3750 m with the CIMEL. 55. This instrument made Sun measurements in four spectral channels. Corresponding variation coefficients of spectral extraterrestrial voltages derived from 17 Langley plots are listed in Table 1. Because of some instrumental problems, sky radiances were not used in our analysis.

CIMEL 13 was relocated to a sea level site on June 24 and stayed there for the duration of the ACE 2 experiment. Unfortunately, the latest dust outbreak took place on July 25 after the experiment was over and only one sunphotometer (at Izana observatory) was still operating.

3. Results

Daily averages for τ_a(500 nm) and their standard deviations are shown in Figure 2a. In conditions of significant diurnal variability we estimated half-day averages where each average was taken over measurements acquired before noon or acquired in the afternoon. These half-day averages are also plotted on Figure 2a. At sea level in the absence of Saharan dust, τ_a(500 nm) was about 0.1, increasing up to 0.4 during dust outbreaks. At higher altitude, 2360 m, the background value of aerosol optical depth at 500 nm was usually smaller than 0.02, growing by an order of magnitude (up to 0.20) in dusty conditions. At the highest elevation (3750 m) where the aerosol optical depth is close to 0.01, the atmosphere can be characterized as very pure and transparent (to obtain τ_a(500 nm) we interpolated between 440 and 670 nm). During Saharan dust events the maximum turbidities occurred on July 8, when daily averaged optical depth was 0.14.

During background conditions at higher elevations, the aerosol optical depth spectra were not well represented by the usual Angstrom ($\lambda^{-\alpha}$) power law because of big relative errors. Nevertheless, the Angstrom parameter can still be considered as a mean indicator of the spectral behavior of aerosol optical depth at sea level. We calculated this parameter using a least squares method in the range 340-1020 nm. Daily (or half-day) averages and their standard deviations are shown in Figure 2b. The Angstrom parameter α, which is indicative of average spectral behavior of aerosol optical depth, displays a significant difference between background and dusty conditions (Figure 2b).

Figure 3 illustrates the diurnal variability of aerosol optical depth at three elevations. Figure 3a depicts typical background conditions. Diurnal variations during the first July Saharan dust outbreak are shown on Figures 3b, 3c and 3d. Dust intervention and disappearance is clearly visible. It is notable that on July 9 at Izana, τ_a was decreasing during the day, whereas at sea level it remained stable. The same decrease was observed at Teide. This suggests that the dust precipitated into the lower atmospheric layer or there is transport out of the upper layer and still transport in to the lower layer at Tenerife or both. Angstrom parameters at Izana and sea level showed practically no variance. It means that even if we had some advection of pollutants or maritime aerosol at sea level it did not play a decisive role in defining optical conditions. In the course of the second dust outbreak on July 17 and 18 (Figures 3e and 3f) the aerosol optical depth varied concurrently at sea level and at higher elevations. Saharan dust advection on July 25 (Figure 3g) illustrates how τ_a varied from the background level up to moderately turbid conditions. Relative diurnal stability of Saharan dust optical properties can be observed in Table 2 (rows in parentheses).

An iterative algorithm developed by *Nakajima et al.* [1983, 1996] was used for retrieving aerosol volume size distributions from spectral sky radiance data. The inversion algorithm produces volume size distributions integrated on the

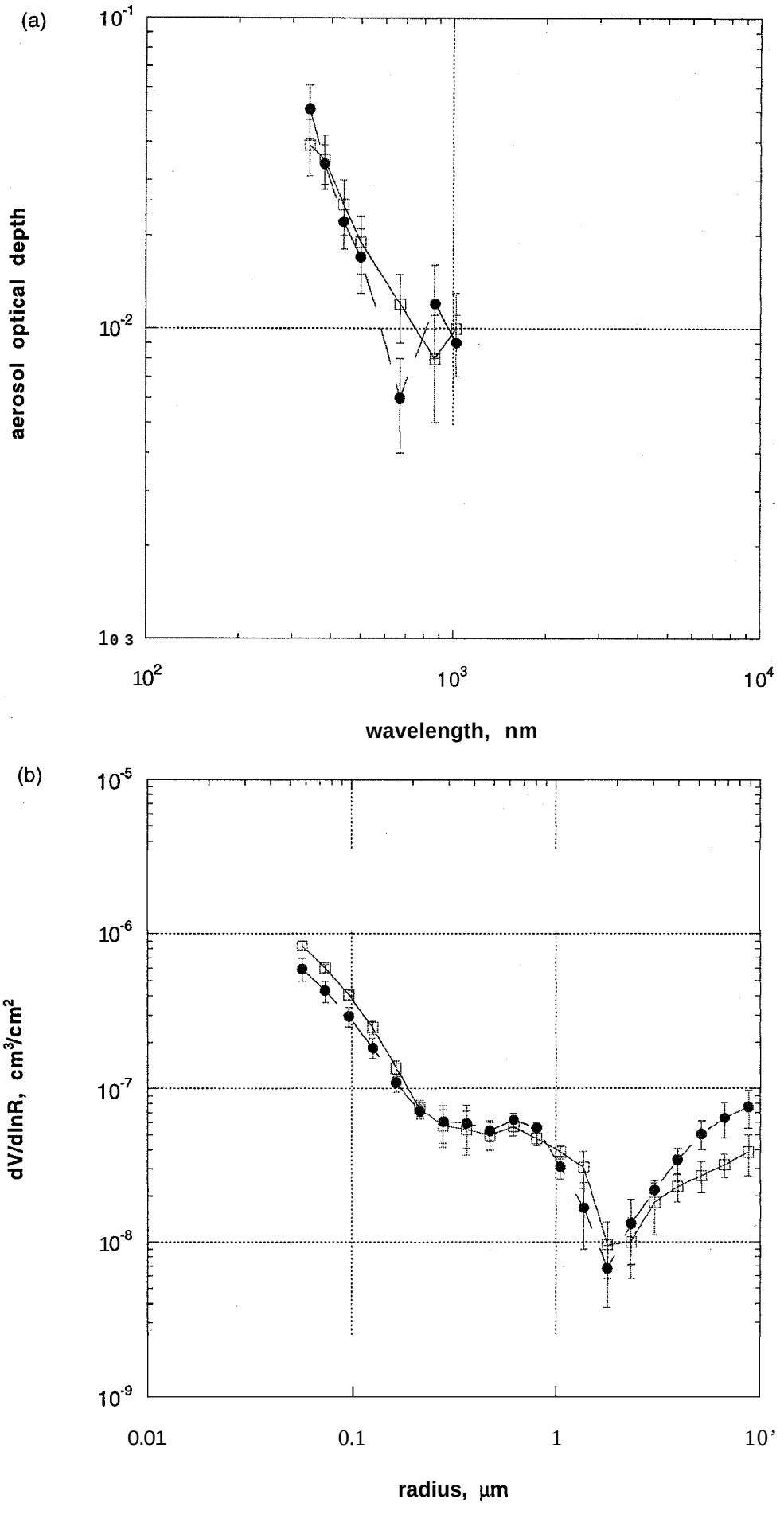

Figure 1. (a) Aerosol optical depth spectra and (b) column volume size distributions measured by colocated sunphotometers at the elevation 2360 m. Solid circles, CIMEL **2,** open squares, CIMEL 13.

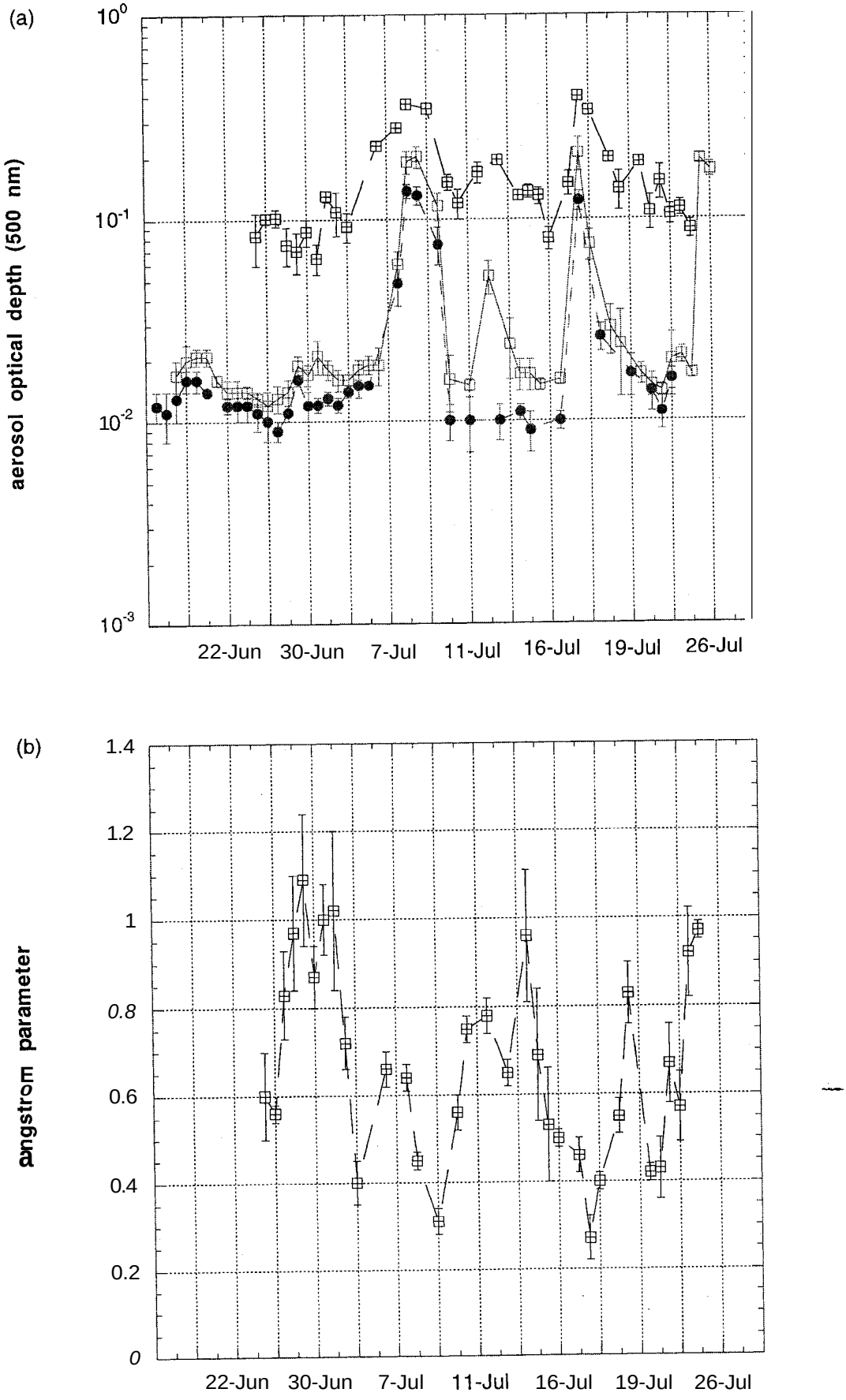

Figure 2. Daily averages of aerosol optical depth at (a) 500 nm and (b) Angstrom parameter. Hatched square, sea level; open square, 2360 m above sea level (asl); solid circles, 3570 m asl.

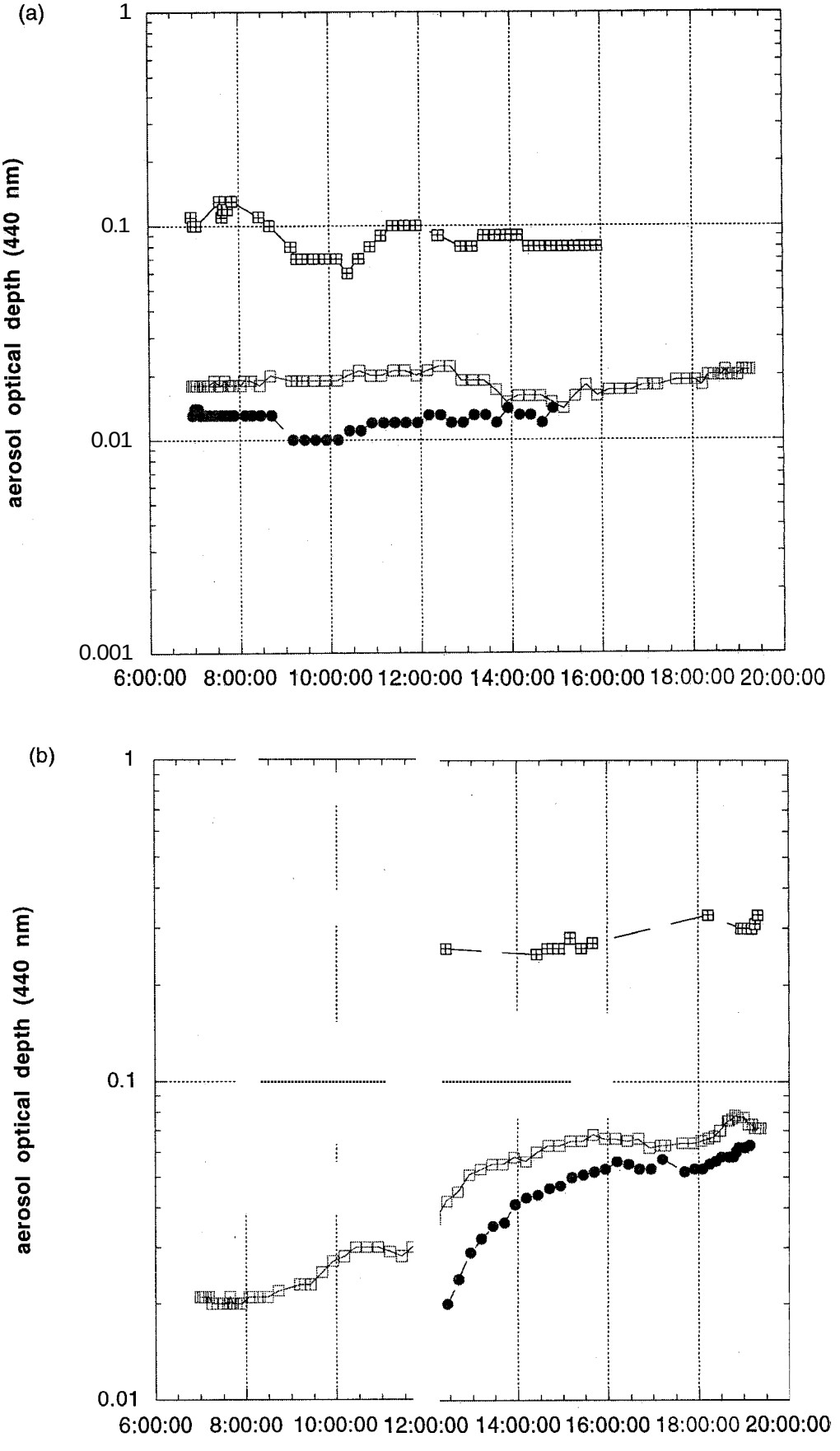

Figure 3. Diurnal variability of aerosol optical depth at 440 nm for three elevations. (a) June 28, (b) July 7, (c) July 8, (d) July 9, (e) July 17, (f) July 18, and (g) July 25. Hatched square, sea level; open square, 2360 m asl; solid circle, 3570 m asl.

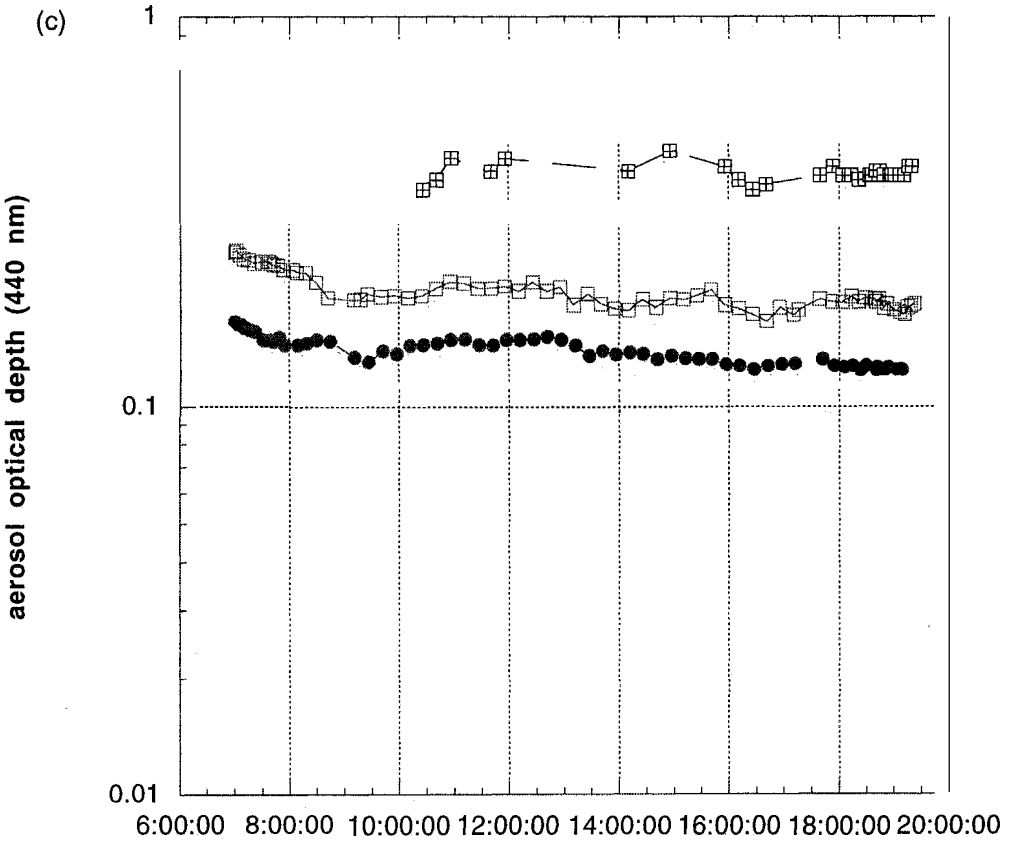

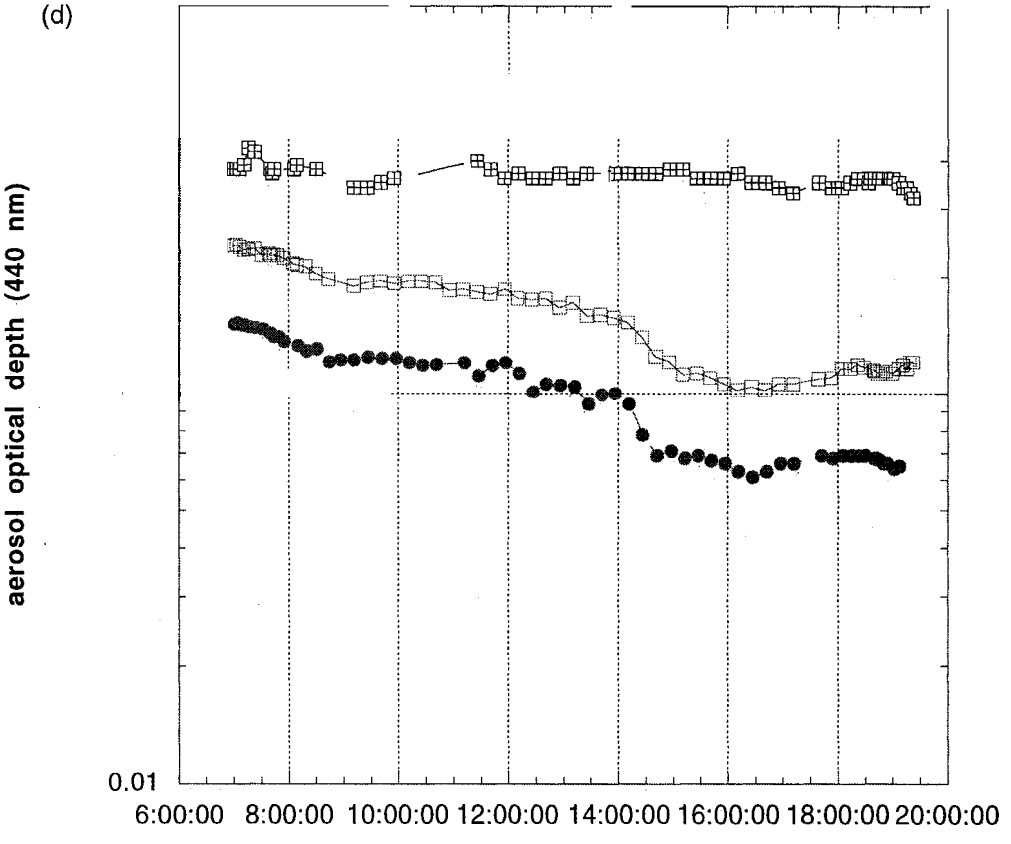

Figure 3. (continued)

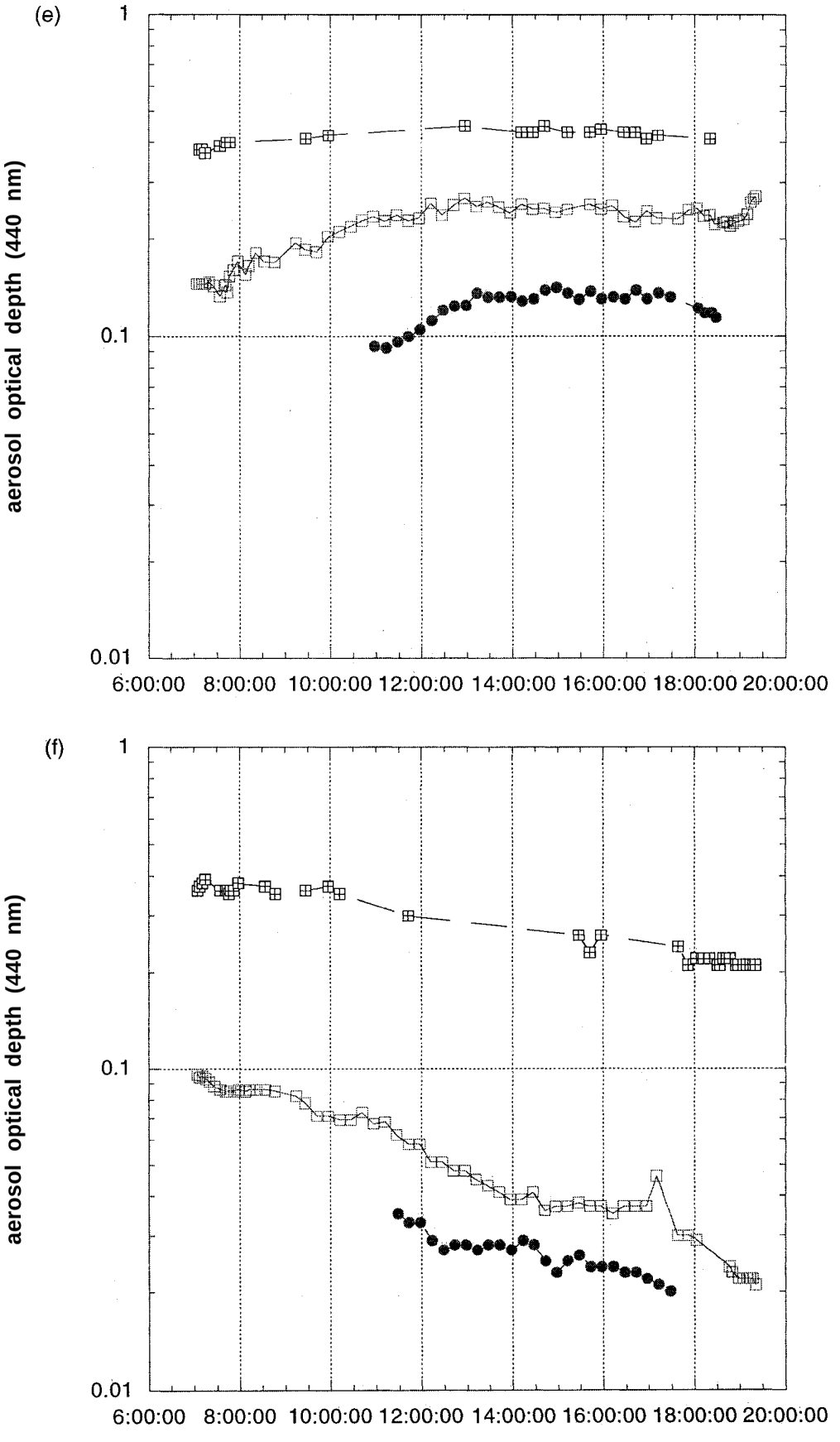

Figure 3. (continued)

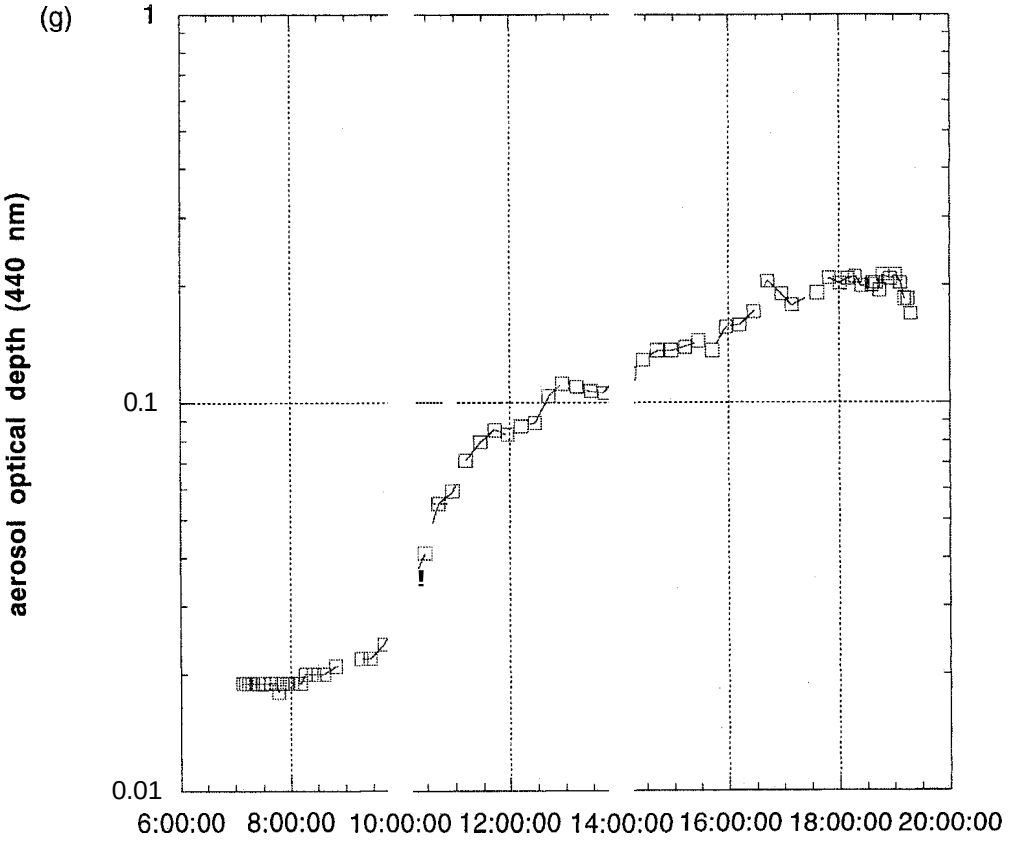

Figure 3. (continued)

Table 2. Variability of Aerosol Optical Depth and Angstrom Parameter in Saharan Dust

Date	Time	Elevation, m	$\tau_a(500)$	σ	τ_a^{min}	τ_a^{max}	a	σ_α	α^{min}	α^{max}
July 7	15:27-19:07	3570	0.05	0.01	0.02	0.06	0.09	0.04	0.01	0.13
July 7	12:55-19:22	2360	0.06	0.01	0.04	0.07	0.43	0.09	0.37	0.67
July 7	1225-19:19	sea level	0.26	0.03	0.22	0.30	0.65	0.03	0.61	0.72
(July 8	07:01-19:13	3570	0.14	0.01	0.12	0.16	0.06	0.03	0.01	0.10)
(July 8	07:00-19:22	2360	0.19	0.02	0.16	0.25	0.22	0.09	0.11	0.39)
(July 8	10:25-19:19	sea level	0.37	0.02	0.34	0.42	0.45	0.02	0.40	0.47)
July 9	07:00-12:00	3570	0.13	0.01	0.12	0.15	0.08	0.03	0.02	0.08
July 9	12:00-19:07	3570	0.08	0.02	0.06	0.11	0.07	0.05	-0.02	0.13
July 9	07:00-12:40	2360	0.20	0.03	0.16	0.24	0.18	0.04	0.13	0.24
July 9	12:55-19:22	2360	0.12	0.02	0.10	0.16	0.25	0.02	0.21	0.29
July 9	07:00-19:22	sea level	0.35	0.02	0.31	0.42	0.31	0.03	0.23	0.40
(July 17	11:00-18:58	3570	0.12	0.01	0.09	0.14	0.06	0.02	0.01	0.10)
July 17	07:00-11:56	2360	0.17	0.03	0.13	0.23	0.20	0.02	0.17	0.24
(July 17	12:11-19:20	2360	0.24	0.01	0.22	0.27	0.16	0.02	0.13	0.22)
July 17	07:07-09:57	sea level	0.38	0.02	0.36	0.40	0.32	0.03	0.27	0.36
(July 17	12:57-18:20	sea level	0.41	0.01	0.40	0.44	0.24	0.02	0.20	0.27)
July 18	11:28-17:28	3570	0.02	0.01	0.02	0.03	0.14	0.05	0.05	0.23
July 18	07:04-11:56	2360	0.08	0.01	0.05	0.09	0.39	0.08	0.31	0.58
July 18	12:11-19:20	2360	0.03	0.01	0.02	0.04	0.77	0.29	0.49	1.34
July 18	07:04-11:42	sea level	0.34	0.02	0.28	0.37	0.40	0.02	0.31	0.42
July 18	15:27-19:20	sea level	0.20	0.01	0.19	0.24	0.55	0.04	0.45	0.58
(July 25	16:40-19:17	2360	0.20	0.01	0.17	0.21	0.14	0.01	0.13	0.17)
(July 26	07:00-07:55	2360	0.17	0.01	0.16	0.19	0.14	0.01	0.14	0.15)

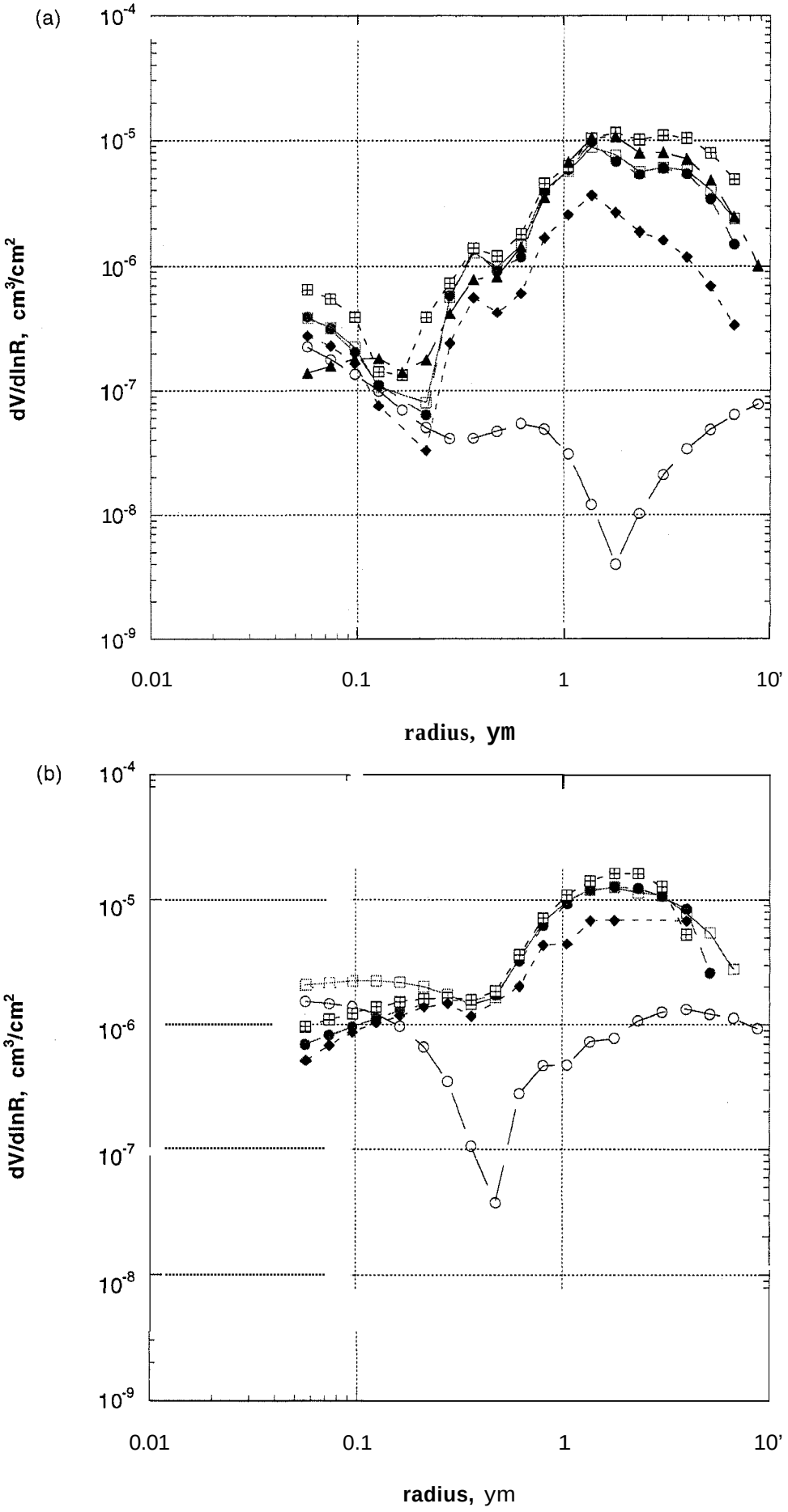

Figure 4. Aerosol volume size distributions in total atmospheric column retrieved from the **sky** almucantar measurements at two elevations: (a) elevation 2360 m, and (b) sea level. Open circle, June 28; open square, July 8; solid circle, July 9; hatched square, July 17; solid diamond, July 18; solid triangle, July 25.

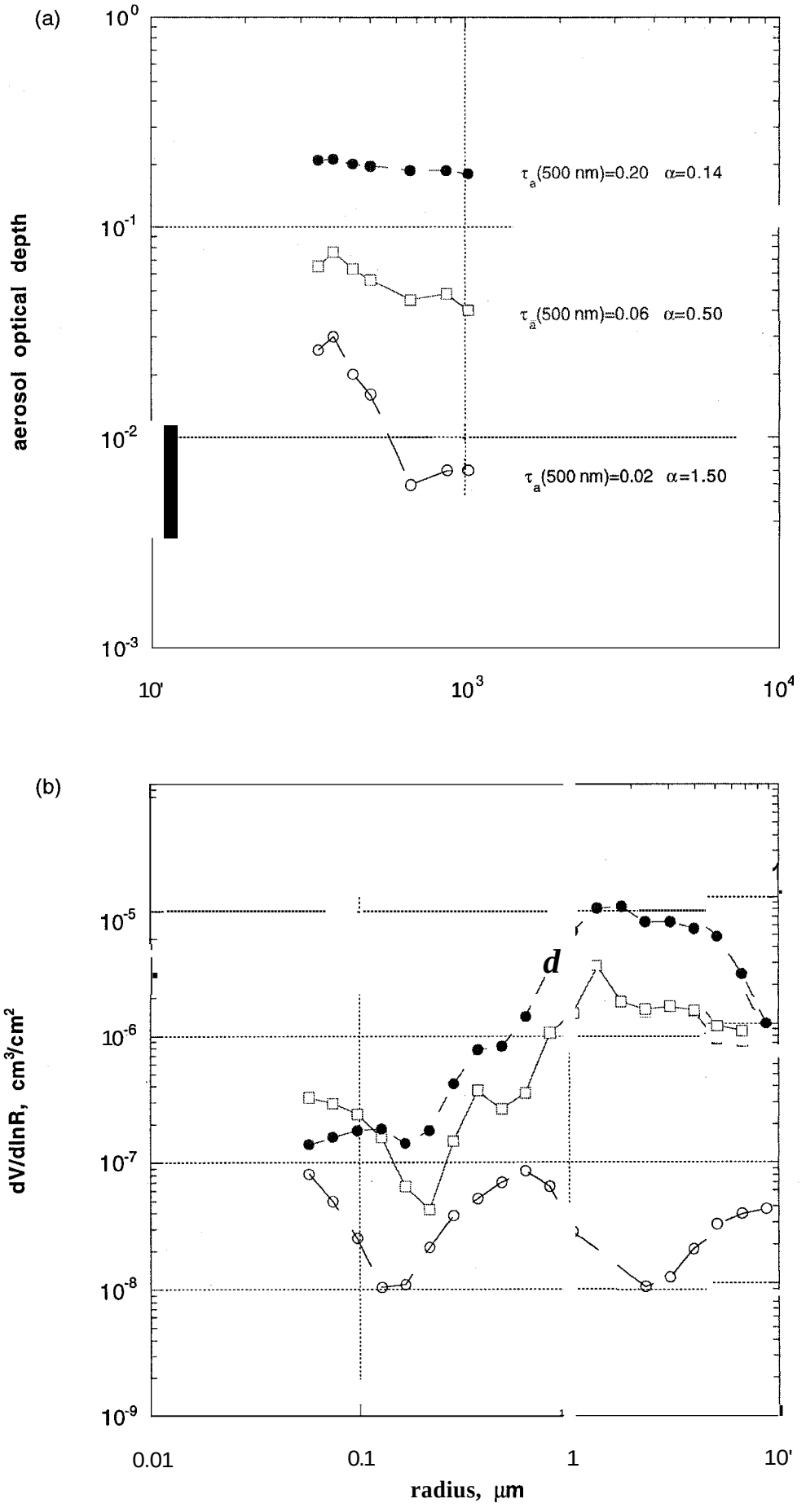

Figure 5. Changes in aerosol optical properties during a Saharan dust intervention, July 25 (elevation 2360 m): (a) aerosol optical depth spectra (open circle, 7:00-10:00; open square, 10:00-12:00; solid circle, 16:40-19:20) and (b) retrieved aerosol volume size distributions (open circle, 7:40-8:50; open square, 11:13; solid circle, 16:40-19:20).

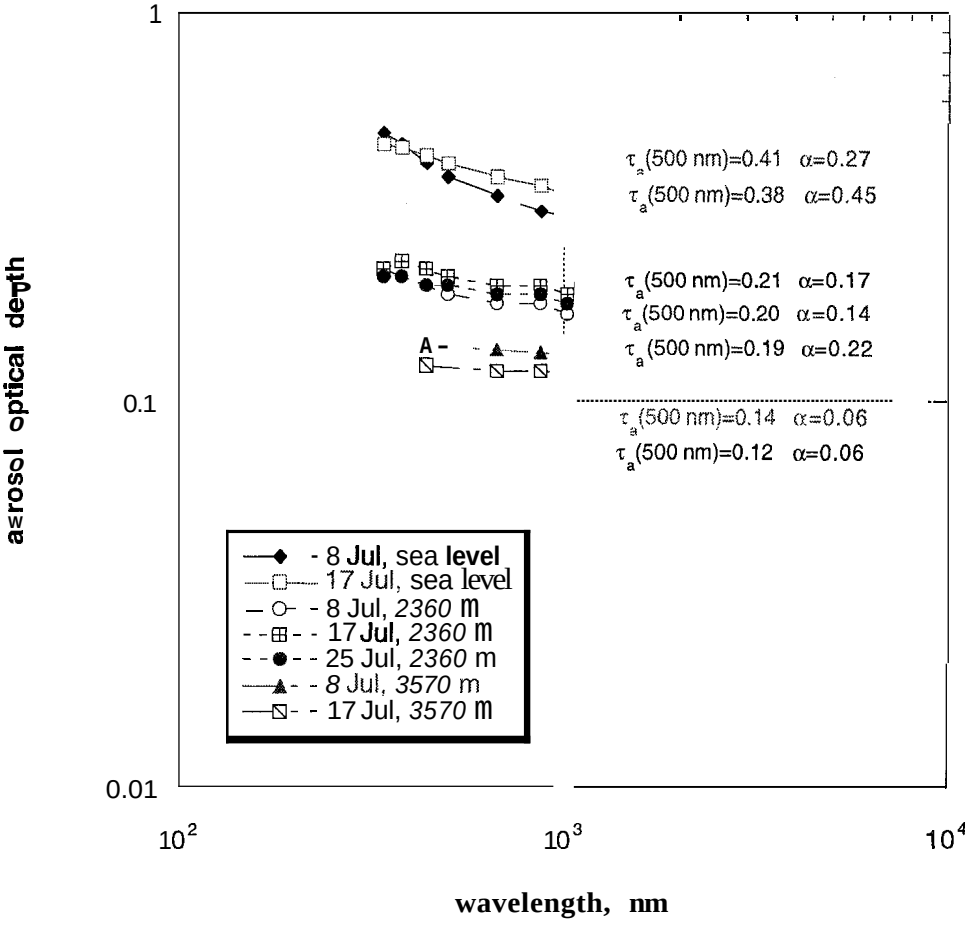

Figure 6. Mean aerosol optical depth spectra at three elevations for three days.

atmospheric column. The two panels illustrate the size distribution in Saharan dust and background conditions at two elevations (Figure 4). Volume size distributions are consistent with the optical depth data and show relative stability between each dust event. Volume size distributions at two heights show that the main portion of coarse particles is situated above 2360 m level. This remains to be corroborated with the lidar observations (E. J. Welton, private communication, 1997).

Measurements made on July 25 clearly demonstrate the changes in aerosol optical properties during a Saharan dust intervention. Incoming dust changed the magnitude and spectral dependence of aerosol optical depth (Figure 5a) and volume spectra of columnar aerosols observed at the height 2360 m above sea level (Figure 5b). During the day the original shape of $\tau_a(\lambda)$ varies with time significantly. Average $\tau_a(500\ \text{nm})$ and corresponding a are listed on Figure 5a. The Angstrom parameter, α, decreases by an order of magnitude from 1.50 in the morning to 0.14 in the late afternoon, which is indicative of additional coarse particles in the atmospheric column. Volume size distributions, retrieved from spectral sky radiance data, demonstrate how the coarse fraction of aerosol associated with the Saharan dust has become dominant (Figure 5b). Thus Figures 5a and 5b are in reasonably good qualitative consistency.

Mean daily spectral extinction for selected days at three elevations emphasize the relative diurnal stability of Saharan dust optical properties (Figure 6). For these days the standard deviations of $\tau_a(500)$ are not higher than 0.02 at sea level and at 2360 m (except for July 17, when σ was 0.03), getting lower (0.012-0.014) at the highest elevation. Angstrom parameters yielded standard deviations between 0.01 and 0.05.

Aerosol optical depth at wavelength 500 nm drops by a factor of 2 as elevation increases up to 2360 m above sea level. The remainder decreases by 40% at elevation 3750 m. Spectral selectivity gradually changes and becomes almost neutral at 3750 m. At the bottom, there is still a lot of submicron aerosol, leading to $a \sim 0.3$-0.4. At Izana there is much less fine particles, thus $a \sim 0.2$. Finally; at Teide only dust is present ($a \sim 0.06$). We can conclude that observational changes are associated with the decrease in columnar number density (aerosol optical depth is an indicator) and, second, with the preservation and dominance of large particles in the aerosol size distribution (smaller Angstrom parameter values as a consequence).

Aerosol optical depths of suspected dust events in the Atlantic Ocean, 200 km northeast of Bermuda and on Bermuda during the Tropospheric Aerosol Radiative Forcing Observational Experiment (TARFOX) in July 1996 [*Smirnov et al.*, 19971 are consistent with the similar weak Atlantic dust episodes in other years reported by *Volgin et al.* [1988], *Reddy et al.* [1990], *Sakerin et al.* [1993], and *Smirnov et al.* [1995] (Figure 7). These measurements were carried out in different

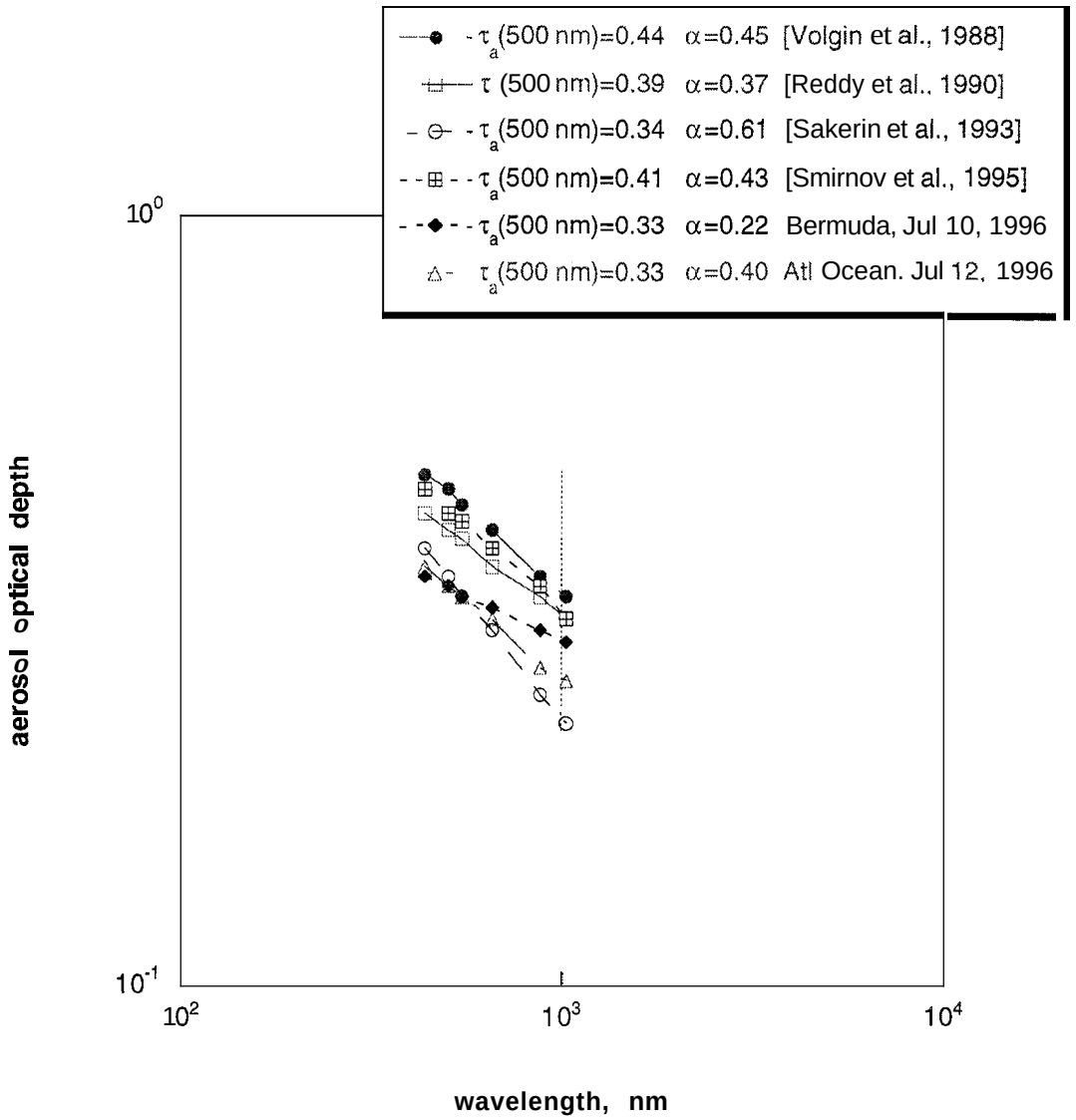

Figure 7. Saharan dust optical properties in Atlantic Ocean.

regions and in various seasons (west coast of Africa, February-March 1986; central Atlantic, August 1988; west coast of Africa, October-November 1989; west coast of Africa, October 1991, correspondingly). In general, mean optical depth and Angstrom parameter values for Saharan dust outbreaks during the ACE 2 experiment are in good agreement with previously reported results *[Volgin et al.*, 1988; *Reddy et al.*, 1990; *Sakerin et al.*, 1993; *Smirnov et al.*, 1995, 19971.

There is a good agreement between ACE-2 data and data obtained on other sites in the AERONET network influenced by Saharan air masses [*Holben et al.,* 19981. Figure 8 presents aerosol optical depth spectra (Figure 8a) and aerosol volume size distributions (Figure 8b) for Dry Tortugas (24'36' N, 82°48′ W), Barbados (13'09' N, 59°30′ W), and our ACE *2* site on Tenerife (sea level, 24°18′ N and 16°30′ W). Presented results are admissable and physically acceptable. Moreover, volume size distributions quantitatively and qualitatively agree with the recent studies by ***Porter*** *and Clarke* [1997].

4. Conclusions

The principal conclusions drawn from our work can be summarized as follows:

1. The results of Sun and sky measurements, acquired during ACE *2,* illustrate the temporal and vertical dynamics of aerosol optical properties (aerosol optical depths, Angstrom parameters, and size distributions) at three elevations in Saharan dust air masses advected from West Africa and background conditions.

2. Volume size distributions are qualitatively consistent with optical depth data and show relative stability between each dust event.

3. There is a good agreement between ACE *2* data, previously reported results for Saharan air masses, and data obtained on certain sites of the AERONET network.

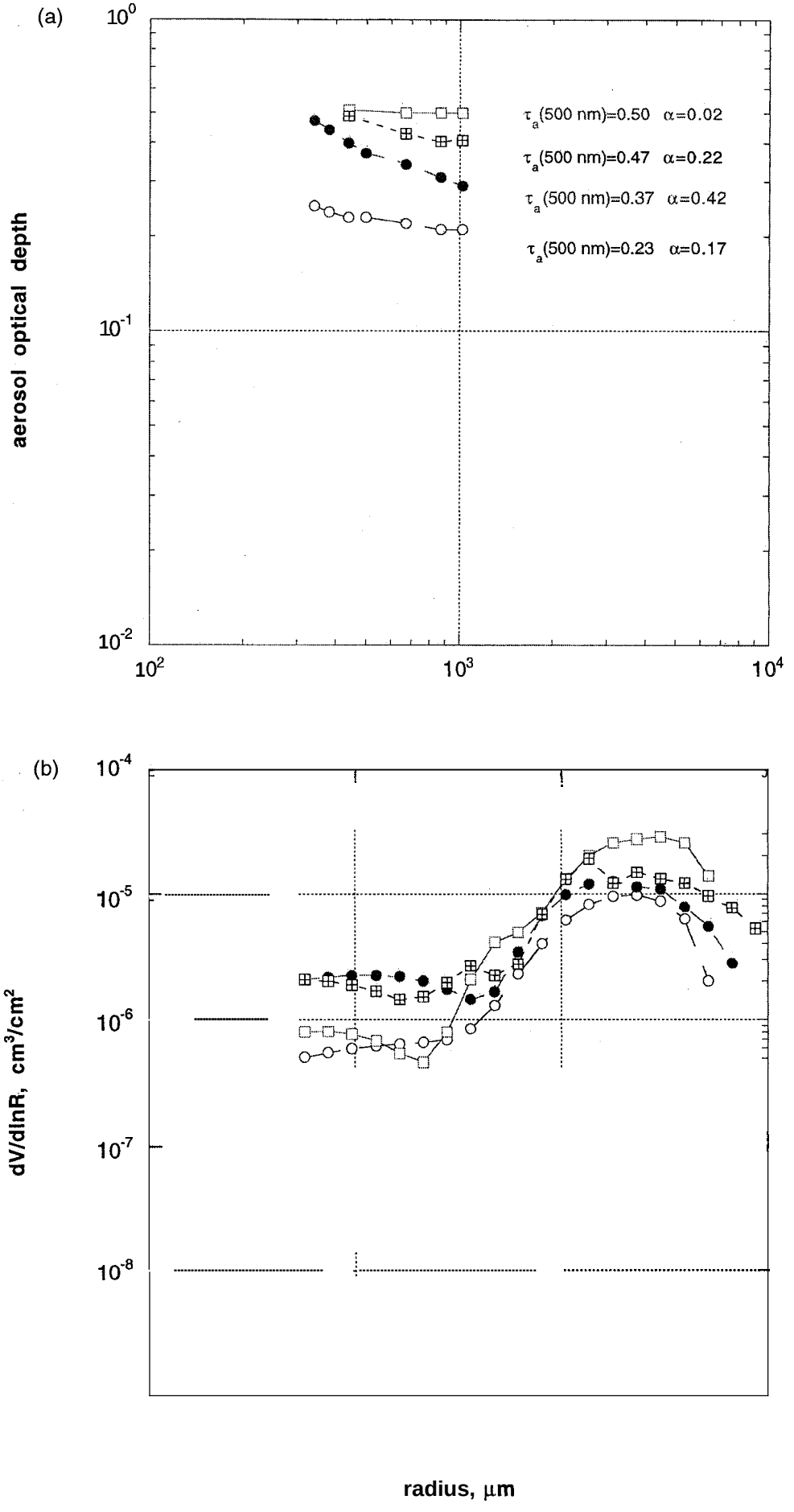

Figure 8. Saharan dust optical properties on the AERONET sites: (a) aerosol optical depth spectra and (b) retrieved aerosol volume size distributions. Open circles, Dry Tortugas, July 7; open squares, Barbados, June 11; solid circles, Tenerife, July 8; hatched squares, Cape Verde, July *26.*

Acknowledgments. The authors thank Dr. Robert Curran of NASA Headquarters and Dr. Michael King of the EOS Project Science Office for their support. The authors would like to thank J. Prospero and M. O. Andreae for useful comments, and R. Fraser, Y. Kaufman and O. Dubovik for fruitful discussions of certain issues.

References

Andreae, M.O., Raising dust in the greenhouse, *Nature*, 380, 389-390, 1996.

Arimoto, R., B.J. Ray, N.F. Lewis, U. Tomza, and R.A. Duce, Mass-particle size distributions of atmospheric dust and the dry deposition of dust to the remote ocean, *J. Geophys. Res.*, 102, 15,867-15,874, 1997.

Holben, B.N., et al., AERONET: A federated instrument network and data archive for aerosol characterization, *Remote Sens. Environ.*, in press, 1998. (Also available on http://spamer.gsfc.nasa.gov.)

Husar, R.B., J.M. Prospero, and L.L. Stowe, Characterization of tropospheric aerosols over the oceans with the NOAA advanced very high resolution radiometer optical thickness operational product, *J. Geophys. Res.*, 102, 16,889-16,909, 1997.

Kaufman, Y.J., A. Gitelson, A. Karnieli, E. Ganor, R.S. Fraser, T. Nakajima, S. Mattoo, and B.N. Holben, Size distribution and scattering phase function of aerosol particles retrieved from sky brightness measurements, *J.Geoph.Res.*, 99, 10,341-10,356, 1994.

Li, X., H. Maring, D. Savoie, K. Voss, and J.M. Prospero, Dominance of mineral dust in aerosol light-scaterring in the North Atlantic trade winds, *Nature, 380*, 416-419, 1996.

Nakajima, T., M. Tanaka and T. Yamauchi, Retrieval of the optical properties of aerosols from aureole and extinction data, *Appl. Opt.*, 22,2951-2959, 1983.

Nakajima, T., G. Tonna, R. Rao, P. Boi, Y. Kaufman and B. Holben, Use of sky brightness measurements from ground for remote sensing of particulate polyispersions, *Appl. Opt.*, 35, 2672-2686, 1996.

Porter, J.N., and A.D. Clarke, Aerosol size distribution models based on in situ measurements, *J. Geophys. Res., 102*, 6035-6045, 1997.

Reddy, P.J., F.W. Kreiner, J.J. DeLuisi, and Y. Kim, Aerosol optical depths over the Atlantic derived from shipboard sunphotometer observations during the 1988 Global Change Expedition, *Global Biogeochem. Cycles, 4*, 225-240, 1990.

Sakerin, S.M., A.M. Ignatov, and D.M. Kabanov, On the correlations in spectral behavior of the aerosol optical depth in some regions of Atlantics, *Atmos. Oceanic Optics*, Engl.Transl., *6*, 526-529, 1993.

Smirnov, A., O. Yershov, and Y. Villevalde, Aerosol optical depth in the Atlantic Ocean and Mediterranean Sea, *Proc. SPIE Int. Soc. Opt. Eng.*, 2582,203-214, 1995.

Smimov, A., B.N. Holben, L. Remer, and I. Slutsker, Measurement of atmospheric optical parameters on East Coast sites, ships and Bermuda (abstract), *Eos, Trans. AGU*, 78 (17), Spring Meet. Suppl., S81, 1997.

Tegen, I., A.A. Lacis, and I. Fung, The influence on climate forcing of mineral aerosols from disturbed soils, *Nature*, 380, 419-422, 1996.

Volgin, V.M., O.A. Yershov, A.V. Smimov, and K.S. Shifrin, Optical depth of aerosol in typical sea areas, *Izv. Acad. Sci. USSR Atmos. Oceanic Phys.*, Engl.Transl., *24*, 772-777, 1988.

P. Formenti, Max Planck Institut fur Chemie, Biochemistry Department, P.O. Box 3060, D-55020 Mainz, Germany.

B.N. Holben, I. Slutsker, and A. Smirnov, Biospheric Sciences Branch, NASA Goddard Space Flight Center, Code 923, Greenbelt, MD 20771. (e-mail: asmirnov@spamer.gsfc.nasa.gov)

E.J.Welton, Physics Department, University of Miami, 1320 Campo Sano Dr., Coral Gables, FL 33146

(Received December 2, 1997; revised May 28, 1998;
accepted May 29, 1998.)